Journal of Molecular Liquids 391 (2023) 123220

Contents lists available at ScienceDirect

Journal of Molecular Liquids

journal homepage: www.elsevier.com/locate/molliq

Hydration structure and dynamics, ultraviolet–visible and fluorescence spectra of caffeine in ambient liquid water. A combined classical molecular dynamics and quantum chemical study

Ioannis Skarmoutsos [a,*], Demeter Tzeli [b,c,*], Ioannis D. Petsalakis [c]

[a] Laboratory of Physical Chemistry, Department of Chemistry, University of Ioannina, 45110 Ioannina, Greece
[b] Department of Chemistry, Laboratory of Physical Chemistry, National & Kapodistrian University of Athens, Panepistimiopolis, 157 71, Athens, Greece
[c] Theoretical and Physical Chemistry Institute, National Hellenic Research Foundation, Vas. Constantinou, 48, GR-116 35, Athens, Greece

ARTICLE INFO

Keywords:
Caffeine
Liquid water
Hydration structure
Classical MD
Time-dependent DFT
UV–Vis Spectroscopy
Fluorescence Spectroscopy
Hydrogen bonding
Reorientational dynamics
Self-Diffusion

ABSTRACT

The hydration structure and related dynamics of caffeine diluted in ambient liquid water have been extensively studied by performing classical molecular dynamics simulations, using our previously developed potential model of caffeine and the TIP4P/2005 water model. The results obtained have revealed that the first hydration shell of caffeine contains on average 56 water molecules. Hydrated caffeine forms in total 3 hydrogen bonds with its neighbor water molecules, with the $O_{caffeine} \cdots H_{water}$ hydrogen bonds exhibiting similar lifetimes with the ones corresponding to $O_{water} \cdots H_{water}$ hydrogen bonds in liquid water. The self-diffusion coefficient of caffeine has been found to be four times lower than the corresponding value for water, being also in agreement with recent experimental measurements. The presence of water molecules inside the solvation shell of caffeine changes significantly their low-frequency intermolecular vibrations, as reflected on the calculated atomic velocity time correlation functions and corresponding spectral densities. Using the estimated average intermolecular structure of the first hydration shell of caffeine, the molecular cluster caffeine@W_{56} was optimized via quantum chemical calculations and subsequently the time-dependent density functional theory was used in order to predict the ultraviolet–visible and fluorescence spectra of hydrated caffeine. The results obtained are in agreement with recent experimental studies, which have proposed that such spectroscopic measurements can be used for the direct determination of alkaloids in aqueous extracts of natural products. In this framework, multi-scale molecular modelling providing accurate predictions of experimental data could also be a very useful tool, linking theoretical physical chemistry with analytical chemistry applications.

1. Introduction

The class of methylxanthines such as caffeine, theophylline and theobromine, which can be found in significant concentrations in natural products [1], are considered as the most widely used alkaloids in a wide range of applications related to the formulation of medicinal products and beverages [2,3]. Among these alkaloids, caffeine is considered as the most consumed substance, due to its ability to stimulate the central nervous system [2]. In this way, caffeine consumption in moderate doses can restore mental alertness or wakefulness during fatigue and drowsiness and has a synergistic effect on pain relief when used in combination with analgesics [4,5].

The concentration of caffeine, or other specific chemical substances in general, in raw natural products is an important factor and often determines not only the basic organoleptic characteristics [6] of energy drinks and beverages, but also the stages in the development of pharmaceutical formulations which ensure the safety and efficacy of the desired medicinal products [7,8]. Therefore, the amount of caffeine in raw natural products should be accurately determined using state-of-the-art physicochemical analytical techniques. Interestingly, recent experimental studies have suggested the use of fluorescence spectroscopic methods to determine alkaloids in aqueous extracts of green coffee beans [9].

From a physicochemical point of view, in order to obtain a deeper understanding of absorption and fluorescence spectra of chromophores in solution it is important to provide further insight on the

* Corresponding authors.
E-mail addresses: iskarmoutsos@uoi.gr (I. Skarmoutsos), tzeli@chem.uoa.gr (D. Tzeli).

https://doi.org/10.1016/j.molliq.2023.123220
Received 25 June 2023; Received in revised form 27 September 2023; Accepted 30 September 2023
Available online 2 October 2023

solute–solvent interactions and the underlying solvation mechanisms, which can affect several spectral characteristics [10–12]. Therefore, the determination of the hydration structure of caffeine and related dynamics in these aqueous extracts can provide important information about the relation between local structural effects and spectroscopic observables in aqueous solutions of caffeine. Moreover, as it has been pointed out in our previous studies, a deeper knowledge of the hydration structure and the translational diffusion of active pharmaceutical ingredients in water can be related to their *in vivo* drug dissolution rate [13].

One of the most important tools used to obtain a fundamental understanding of molecular-scale phenomena in condensed matter systems and to improve the design of modern technologies with applications in energy, nanoscience, engineering and biomedical science is molecular modeling and simulation [14]. Multi-scale molecular modeling techniques [15] are considered to have high predictive capabilities of the properties of molecular systems, which arise from physicochemical phenomena on multiple length and time scales.

In the present study, our main aim was to employ multi-scale molecular simulation techniques, ranging from atomistic classical molecular dynamics (MD) to time-dependent density functional theory (TD-DFT) calculations to determine the hydration structure and related dynamics of caffeine in ambient liquid water and then to calculate the ultraviolet–visible (UV–Vis) and fluorescence spectra of caffeine in solution. In our recent studies [16], we developed a force-field for caffeine using quantum chemical calculations in order to study the ethanol cosolvent effect in supercritical CO_2 on the solvation structure and dynamics of caffeine in the mixed CO_2-ethanol supercritical solvent. Using this newly developed force field, as well as one of the most popular force fields used to model the properties of ambient liquid water (TIP4P-2005) [17] we investigated the solvation structure and related dynamics of caffeine diluted in water via classical MD simulations. Subsequently, the most representative configurations, corresponding to the average calculated intermolecular structure of the first hydration shell of caffeine, were used in our TD-DFT calculations in order to calculate the UV–Vis and fluorescence spectra of hydrated caffeine. Note that the main aim of the present study is to explore in detail the hydration structure of caffeine diluted in water, focusing on the possible existence of preferential interactions among the different interaction sites of caffeine and water (such as e.g. hydrogen bonding interactions) and then to investigate the effect of these interactions on the electronic spectra of hydrated caffeine, such as the UV–Vis and fluorescence spectra. For this reason, in this first approach we focused on dilute solutions of caffeine in water and not on aqueous solutions of higher concentrations of caffeine. Among several multi-scale computational studies on caffeine-water interactions reported in the literature [18–26], previous simulation studies revealed that aggregation phenomena between the caffeine molecules are important [23–26], indicating that dilute solutions of caffeine are the most appropriate ones if someone focuses mainly on caffeine-water interactions. In general, our treatment can be considered as the first step towards a further development of multi-scale computational methods in order to link molecular simulations with experimental spectroscopic measurements used for the direct determination of alkaloids in aqueous extracts of natural products.

2. Computational methods

Classical MD simulations of a system containing one caffeine molecule dissolved in 499 water molecules at 298.15 K in a cubic simulation box were performed with the DL_POLY code [27]. The initial configuration of the system was prepared with the *packmol* software [28], with box dimensions corresponding to the experimental density of liquid water at 1 bar. The simulated mixture was initially equilibrated at the canonical (NVT) ensemble for 1 ns, using the potential model developed for caffeine in our previous studies [16] and the TIP4P-2005 potential model of water [17]. The Lennard-Jones parameters used to describe the interactions among caffeine and water have been estimated using the Lorentz-Berthelot combination rules [14]. Subsequently, a simulation at the isothermal-isobaric (NPT) ensemble for $P = 1$ bar was performed for a period of 5 ns, to estimate the density of the system. Using the calculated density of the mixture, a second equilibration run at the canonical ensemble was performed for 2 ns. Finally, a 10 ns NVT-MD production run was performed in order to calculate the properties of the system.

The equations of motion were integrated using a leapfrog-type Verlet algorithm [14] and the integration time step was set to 1.0 fs. The Nose-Hoover thermostat [29] and barostat [30] with a temperature and pressure relaxation time of 0.5 ps, respectively, were used to constrain the temperature and the pressure during the simulations. A cut-off radius $r_c = 12.0$ Å has been applied to the Lennard Jones interactions, and long-range corrections have been considered, while the Ewald summation technique [14] has been used to account for the long-range electrostatic interactions.

The caffeine hydration and the corresponding absorption and emission spectra of hydrated caffeine were also investigated via DFT/TD-DFT calculations using the B3LYP [31,32] and M06-2X [33] functionals in conjunction with the 6-31G(d,p) [34] and Def2TZVP [35] basis sets. In order to directly link the quantum chemical calculations with the classical MD simulations, representative configurations of the first hydration shell of caffeine were taken from the MD simulation trajectory, where all the water molecules being inside the first hydration shell of caffeine were explicitly added. Note that the selected configurations contained 56 water molecules around caffeine, which corresponds to the calculated average coordination number of the first hydration shell of caffeine from our MD simulations, and also exhibited the same average structural features revealed by these simulations. In order to further investigate the effects of different quantum chemical methodologies on the results obtained, several approaches were also tested in the framework of the present study. In this respect, the water solvent was also included implicitly, using the dielectric constant of the solvent and employing the polarizable continuum model (PCM) [36,37], both implicitly and explicitly. In the latter approach, initially the caffeine molecule was energetically optimized, including the solvent implicitly via the PCM model. Then, the caffeine molecule within its first hydration shell, containing 56 water molecules, were energetically optimized at ONIOM multi-scale methodology [38] with and without the implicit inclusion of the water solvent. ONIOM is a hybrid multi-scale methodology, which treats different parts of a molecular system with different methodologies, such as ab initio, semi-empirical, or molecular mechanics methods in order to produce reliable intra- and inter-molecular geometries and energies at reduced computational cost [38]. The most important part of the system is called model system and the remaining system corresponds to the environment system. The small “model” part is treated with an accurate and more expensive method, usually a quantum mechanical (QM) method such as DFT, while the remaining part “environment” is treated with a less accurate method, but still efficient method such as semiempirical QM or classical molecular mechanics.

Here, the ONIOM(M06-2X:PM6) and ONIOM(B3LYP:PM6) methodologies were used. The calculated system is divided in two layers, the first layer is the caffeine molecule which is calculated at the DFT methodology, and the second layer consists of the 56 water molecules calculated at the semi-empirical PM6 methodology. The geometry of both layers was geometry optimized at the multi-scale ONIOM level.

In all cases, the absorption and emission spectra of the caffeine molecule were calculated via the TD-DFT methodology including the 40 lowest-in-energy excited singlet-spin electronic states. For the plot of the spectra, the half width at half height was 0.2 eV. All calculations were carried out employing the Gaussian16 program. [39].

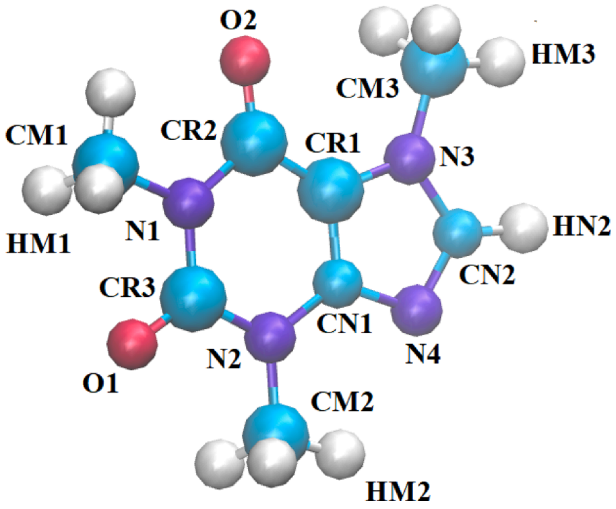

Fig. 1. Different atom types of caffeine in the employed force field.

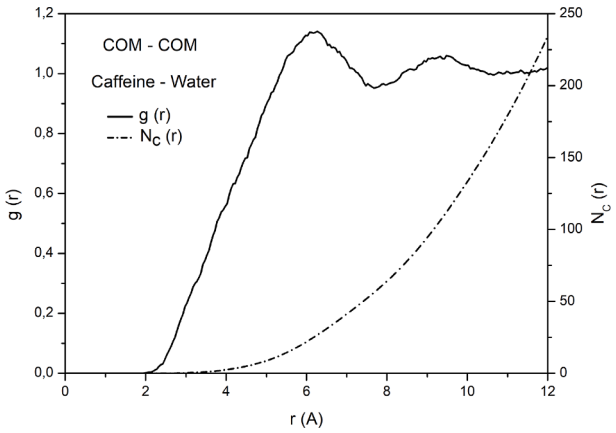

Fig. 2. The calculated caffeine-water COM-COM RDF and the radial dependence of the corresponding coordination number N_c (r).

3. Results and discussion

3.1. Local hydration structure – Hydrogen bonding

The local intermolecular structure in the system was investigated in terms of the center of mass (COM) - (COM) and atom–atom pair radial distribution functions (RDF). The different atom types of caffeine in the employed force field are depicted in Fig. 1. The calculated caffeine-water COM-COM RDF and the radial dependence of the corresponding coordination number N_c (r) are presented in Fig. 2. From this figure it can be observed that the caffeine -water COM-COM RDF exhibits a maximum at 6.28 Å, followed by a minimum located at 7.68 Å, which corresponds to the size of the first hydration shell of caffeine. The calculated coordination number corresponding to the first hydration shell of caffeine is 56.08, signifying that the hydration shell of caffeine, which has a radius of 7.68 Å, consists on average of 56 water molecules.

The local orientational structure around hydrated caffeine and preferential hydrogen bonding (HB) interactions between specific interaction sites of caffeine with water molecules have also been investigated in terms of the atom–atom RDF. The most representative RDF are presented in Fig. 3. From the shape of these RDF, it can be clearly seen that hydrated caffeine acts as a hydrogen bond acceptor and forms hydrogen bonds with the surrounding water molecules inside the first hydration shell using its the O1, O2 and N4 atoms. These interactions are reflected on the peaks of the O1-H_w and O2-H_w RDF,

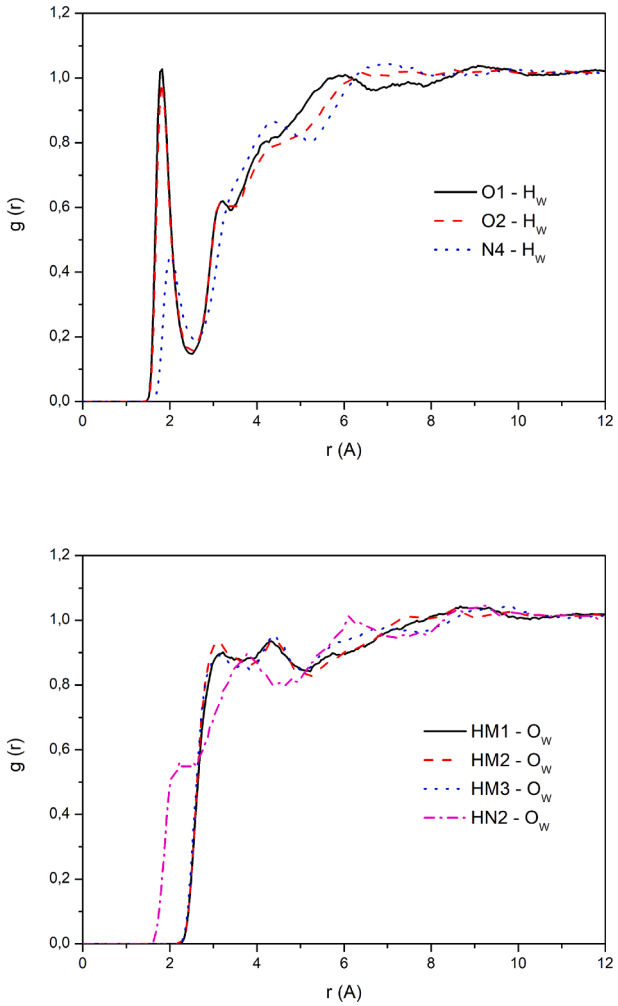

Fig. 3. Calculated representative atom–atom RDF.

located at the very short distance of about 1.83 Å, as well as on the peak of the N4-H_w RDF located at 2.03 Å. On the other hand, the HB interactions between caffeine and water when caffeine acts as HB donor are weaker. These weak interactions are also reflected on the shape of the methyl hydrogen (HM1, HM2, HM3)-O_w and the HN2-O_w RDF, which exhibit either small, non-sharp peaks (in the case of the methyl hydrogen – O_w RDF), or weak shoulders (in the case of the HN2-O_w RDF at distances which are longer when compared with the ones corresponding to the peak positions of the O1-H_w, O2-H_w and N4-H_w RDF. For instance, the peaks of the (HM1, HM2, HM3)-O_w RDF are located at about 3.1 Å, whereas the shoulder of the HN2-O_w RDF is located around 2.4 Å. These features are clear indications of the weak HB interactions between caffeine and water, when caffeine acts as a HB donor.

To provide a more quantitative description of the preferential HB interactions between hydrated caffeine and its neighbor water molecules, a hydrogen bond analysis based on geometric criteria was employed. Note that the use of geometric criteria to investigate the existence of hydrogen bonds in liquid water and aqueous solutions is a standard approach in molecular simulations, provide accurate descriptions of the static and dynamic behavior of the HB networks in these systems [13,40–46]. According to the criteria used in the present study, a hydrogen bond between a caffeine HB acceptor atom X (O1, O2 or N4) and a hydrogen atom of water exists if the interatomic distances are defined as follows: d(X…H_w) ⩽ 2.5 Å, d(X… O_w) ⩽ 3.2 Å and the donor–acceptor angle θ = H_w – O_w … X such as θ ⩽ 30° (note also that the symbol – corresponds to intramolecular vectors and the symbol … to intermolecular ones). The cut-off distances in the criterion are

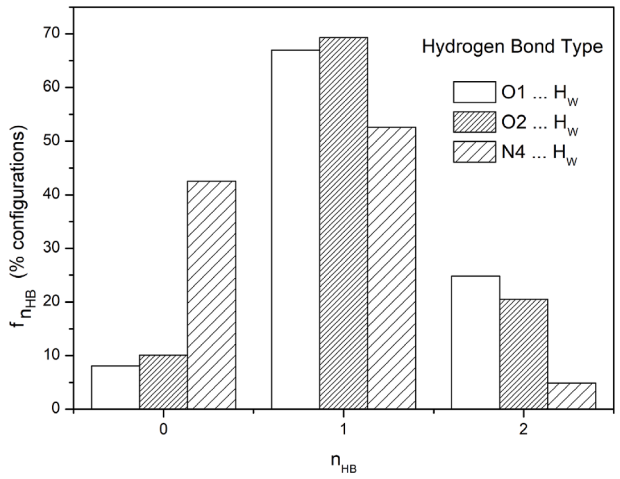

Fig. 4. Calculated fractions of configurations where the hydrated caffeine molecule forms 0,1 or 2 hydrogen bonds of each of the three investigated predominant types (O1…H_w, O2…H_w and N4…H_w).

determined by the location of the minima of the corresponding RDF.

The calculated fractions of configurations where the hydrated caffeine molecule forms 0,1 or 2 hydrogen bonds of each of the three investigated predominant types (O1…H_w, O2…H_w and N4…H_w) are presented in Fig. 4. From this figure it can be observed that in the cases of the O1…H_w and O2…H_w hydrogen bonds, in a significant fraction of configurations (about 66.5 and 68.5 %, respectively) caffeine forms one bond of these types. The fraction of configurations where caffeine forms two hydrogen bonds of these types (O1…H_w and O2…H_w) is also non negligible (about 25.9 and 22.5 %, respectively), leading to the average numbers of about 1.18 O1…H_w hydrogen bonds and 1.14 O2…H_w hydrogen bonds per caffeine molecule. On the other hand, the fraction of configurations where caffeine forms one and two N4…H_w hydrogen bonds are lower (about 55.1 and 4.6 %, respectively) leading to the average numbers of about 0.64 N4…H_w hydrogen bonds per caffeine molecule. In general, we may conclude that in the most predominant local hydration structures of caffeine, caffeine forms three hydrogen bonds with its neighbour water molecules which are inside the first hydration shell. These hydrogen bonds correspond to the O1…H_w, O2…H_w and N4…H_w hydrogen bond types, where caffeine acts as a hydrogen bond acceptor.

3.2. Hydrogen bond dynamics

Apart from the static description of the investigated types of hydrogen bond formed among caffeine and the neighbor water molecules (O1 … H_W, O2 … H_W and N4 … H_W), their dynamics were also investigated in terms of the corresponding $C_{HB}(t)$ time correlation functions (TCF) [47–50]:

$$C_{HB}(t) = \frac{\langle \delta h_{ij}(0) \cdot \delta h_{ij}(t) \rangle_{t^*}}{\langle \delta h_{ij}(0)^2 \rangle}, \; \delta h_{ij}(t) = h_{ij}(t) - \langle h_{ij} \rangle \quad (1)$$

The variable h_{ij} is such as $h_{ij}(t) = 1$ when a hydrogen atom j of a water molecule is hydrogen bonded with a HB acceptor atom X (O1, O2 or N4) i of caffeine at times 0 and t, and the corresponding hydrogen bond has not been broken in the meantime for a period longer than t*, otherwise, $h_{ij}(t) = 0$. The case where $t^* = 0$ corresponds to the continuous HB dynamics, and the one where $t^* = \infty$ corresponds to the intermittent HB dynamics. These two definitions describe very different aspects of HB dynamics. According to the continuous definition, the breaking of a hydrogen bond during the time interval [0, t] is not allowed and the continuous lifetime is the time required for the first breaking of a bond created at time t = 0. On the other hand, in the intermittent case the persistence probability at time t of a hydrogen bond created at t = 0 is investigated, regardless of multiple breakings and reformations of this bond during the time interval [0, t]. The calculated continuous and intermittent TCF $C^C_{HB}(t)$ and $C^I_{HB}(t)$ for all the investigated types of hydrogen bonds are presented in Fig. 5. As the system size increases $\langle h_{ij} \rangle \rightarrow 0$ and at the infinite size limit it approaches the zero value. In the case where $\langle h_{ij} \rangle \simeq 0$ equation (1) can be expressed as:

$$C_{HB}(t) = \frac{\langle h_{ij}(0) \cdot h_{ij}(t) \rangle_{t^*}}{\langle h_{ij}(0)^2 \rangle} \quad (2)$$

The HB lifetime τ_{HB} is defined as:

$$\tau_{HB} = \int_0^\infty C_{HB}(t) \cdot dt \quad (3)$$

The calculated continuous and intermittent HB lifetimes are also

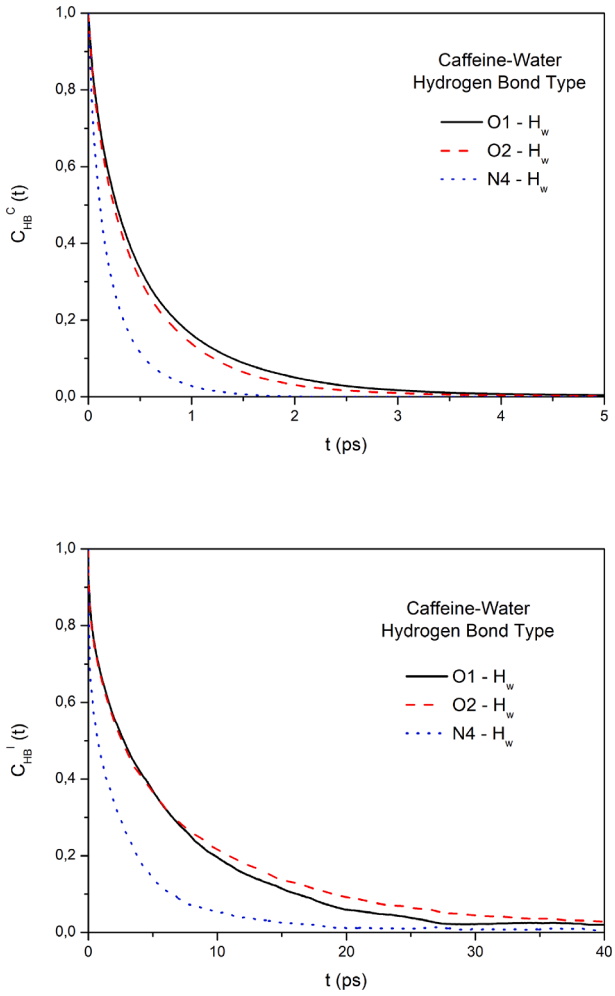

Fig. 5. Calculated continuous and intermittent TCF $C^C_{HB}(t)$ and $C^I_{HB}(t)$ for all the investigated types of hydrogen bonds.

Table 1
Calculated continuous and intermittent hydrogen bond lifetimes for the O1 … H_W, O2 … H_W and N4 … H_W hydrogen bond types.

Hydrogen Bond Type	τ^C_{HB}(ps)	τ^I_{HB}(ps)
O1 … H_W	0.55	6.15
O2 … H_W	0.48	6.88
N4 … H_W	0.22	2.62

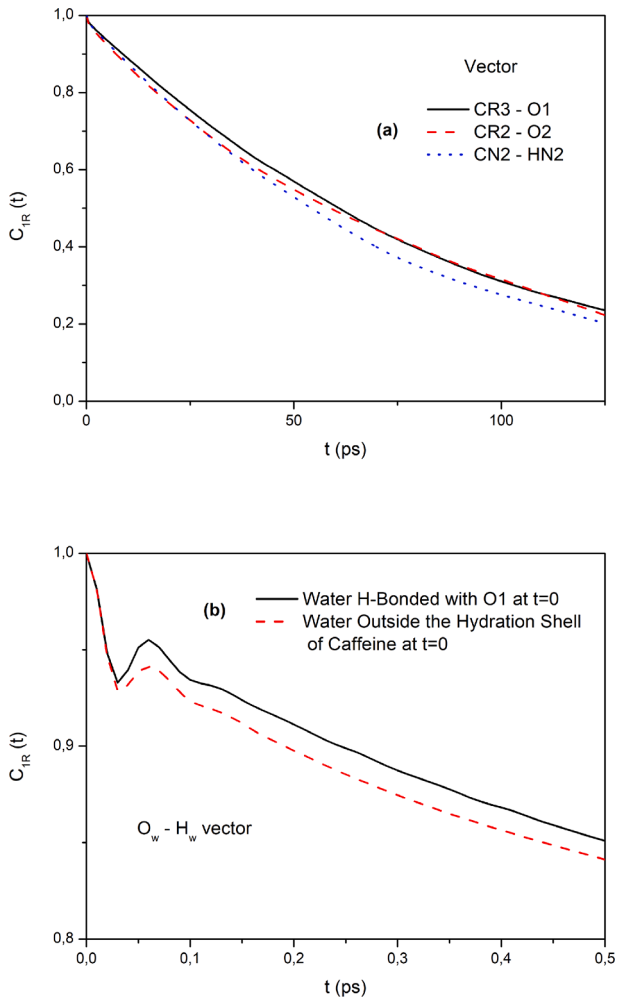

Fig. 6. (a) Calculated first order Legendre reorientational TCF, $C_{1R}(t)$, for the CR3 - O1, CR2 - O2 and CN2 - HN2 intramolecular vectors of caffeine. **(b)** Calculated $C_{1R}(t)$ reorientational TCF for the O_w - H_w vector of water molecules which at t = 0 are. i) Hydrogen bonded to O1 of caffeine and ii) Outside the solvation shell of caffeine.

presented in Table 1, where it can be clearly seen that the continuous and intermittent lifetimes of the O1 … H_W and O2 … H_W hydrogen bonds are quite similar and much longer in comparison with the ones corresponding to the N4 … H_W hydrogen bond. As also observed in our previous studies on the hydration of favipiravir in ambient liquid water [13], the $O_{caffeine}$ … H_{water} hydrogen bonds exhibit similar lifetimes with the ones corresponding to O_{water} … H_{water} hydrogen bonds in liquid water.

3.3. Reorientational -translational dynamics

Reorientational dynamics in liquids can be efficiently characterized in terms of the well-known Legendre reorientational TCF of selected intra molecular vectors:

$$C_{\ell R}(t) = P_\ell\langle\vec{u_i}(0)\cdot\vec{u_i}(t)\rangle \quad (4)$$

here, $\vec{u_i}$ is a normalized vector associated to molecule i, and P_ℓ is a Legendre polynomial of order ℓ. In the present study, we focused on the reorientational dynamics of particular representative intramolecular vectors of caffeine, which are related to HB interactions among caffeine and water molecules. In this respect the calculated first order Legendre reorientational TCF, $C_{1R}(t)$, for the CR3 - O1, CR2 - O2 and CN2 - HN2 intramolecular vectors of caffeine are presented in Fig. 6a. In order to also the investigate the effect of HB interactions with caffeine on the reorientational dynamics of the water molecules the $C_{1R}(t)$ reorientational TCF for the O_w - H_w vector of water molecules was investigated for two different cases: i) For water molecules which at t = 0 are hydrogen bonded to O1 of caffeine and ii) For water molecules which at t = 0 are outside the solvation shell of caffeine. The results obtained are presented in Fig. 6b. From Fig. 6 we may conclude that the reorientational dynamics of caffeine is slower and also that the HB interactions between water and caffeine affect the short-time reorientational dynamics. The latter is characterized by the well-known minima and maxima of the Legendre reorientational TCF at very short-time scales up to 0.1 ps and, according to the literature, is related to a molecular jump mechanism of water reorientation [51–53]. As it can be seen in Fig. 6b, these local extrema are more pronounced, with more abrupt changes observed, when water interacts with caffeine via HB interactions, signifying a more hindered rotation of water molecules inside the solvation shell of caffeine. At longer time scales the decay of $C_{1R}(t)$ for water molecules outside the solvation shell of caffeine at t = 0 is slightly faster, signifying a slowing-down of water reorientational dynamics when they form hydrogen bonds with caffeine inside its hydration shell. The differences in the reorientational dynamics of caffeine and the water molecules which are hydrogen-bonded to caffeine or outside its hydration shell can be more quantitatively presented in terms of the calculated Legendre reorientational correlation times, using the relation:

$$\tau_{\ell R} = \int_0^\infty C_{\ell R}(t)\cdot dt \quad (5)$$

We noticed that the decay of $C_{1R}(t)$ for the investigated intramolecular vectors of caffeine can be very well described in terms of an exponential decay function, $\exp(-t/\tau)$, where in that case the calculated decay time τ is equal to τ_{1R}. The estimated values of τ_{1R} for the CR3 - O1, CR2 - O2 and CN2 - HN2 intramolecular vectors of caffeine are 85.5, 80.2 and 76.7 ps, respectively. The decay of $C_{1R}(t)$ for the the O_w - H_w vector of water can be better described by a sum of three exponential decay functions and the estimated values of τ_{1R} for water molecules hydrogen-bonded with the O1 of caffeine or being outside the first hydration shell of caffeine at t = 0 are 7.0 and 6.6 ps, respectively. From these results it can be clearly observed that the reorientation of hydrated caffeine is much slower in comparison with water, which is clearly reflected on the one order of magnitude difference in the calculated reorientational correlation times of caffeine and water. Moreover, the HB interactions of water molecules with caffeine promote more abrupt changes in the short-time reorientational dynamics of water. These changes indicate that the rotation of water molecules which interact with caffeine via HB interactions is more hindered in comparison with the rotation of bulk water molecules, although it is well known that the HB interactions among water molecules also affect their reorientational dynamics [54]. This effect of the water-caffeine HB interactions on water reorientation is also reflected on the shorter calculated first-order Legendre reorientational correlation times τ_{1R} of water molecules being outside the first hydration shell of caffeine.

The translational dynamics of caffeine and water molecules have also been investigated in terms of the COM and representative atomic velocity TCF:

$$C_v^i(t) = \frac{\left\langle \vec{v}_i(0)\cdot\vec{v}_i(t)\right\rangle}{\left\langle \vec{v}_i(0)^2\right\rangle} \quad (6)$$

with the associated spectral densities, $S_v^i(\omega)$, calculated by performing a Fourier transform

$$S_v^i(\omega) = \int_0^\infty \cos(\omega\cdot t)\cdot C_v^i(t)\cdot dt \quad (7)$$

here, the $S_v^i(\omega)$ have been calculated by numerical integration using a

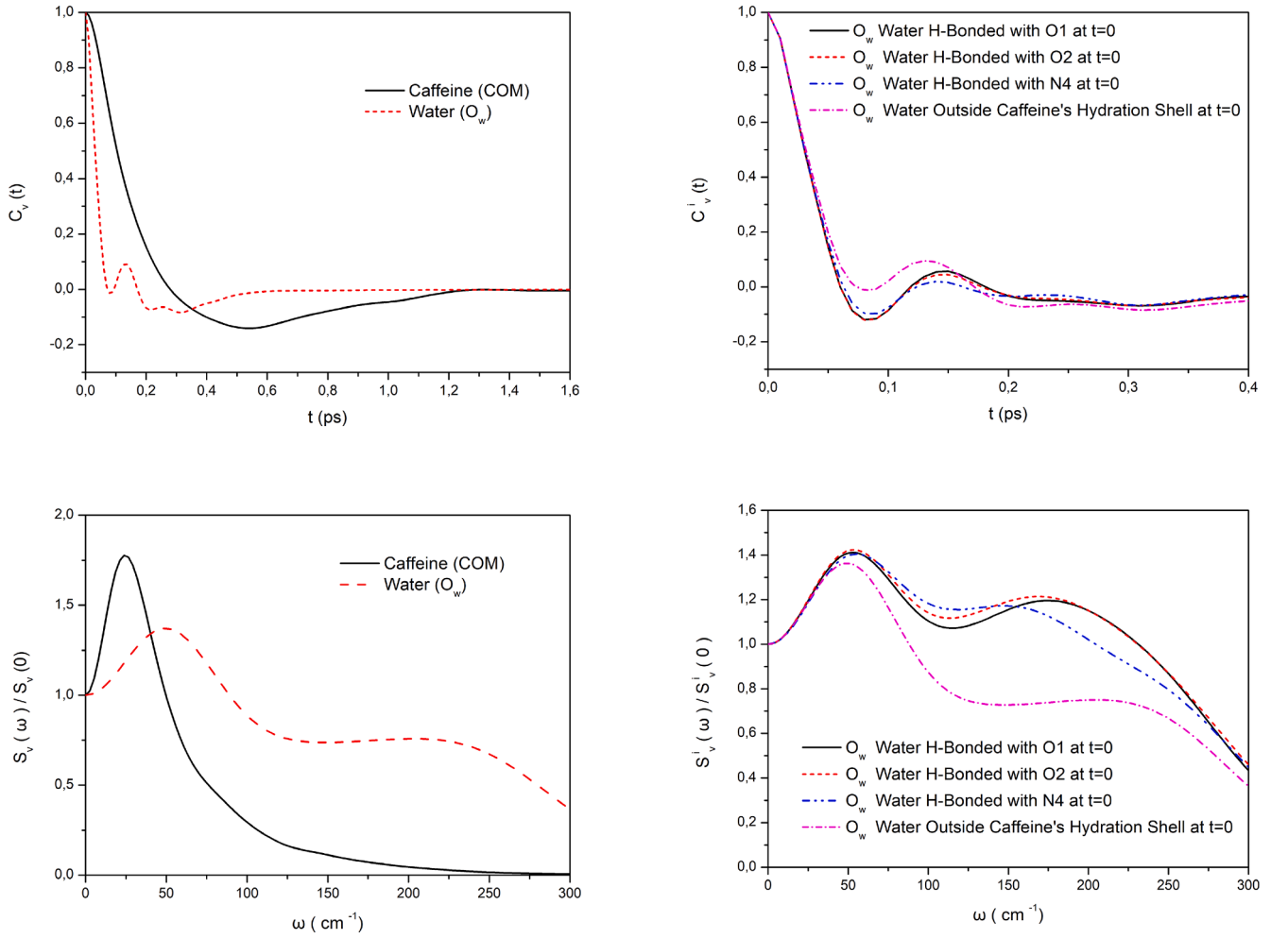

Fig. 7. Calculated normalized COM velocity TCF of caffeine and the oxygen velocity TCF of water, together with their associated normalized spectral densities $S_v^i(\omega)/S_v^i(0)$.

Fig. 8. Calculated normalized oxygen velocity TCF and corresponding normalized spectral densities of water molecules which at t = 0 are i) hydrogen-bonded with O1 of caffeine, ii) hydrogen-bonded with O2 of caffeine, iii) hydrogen-bonded with N4 of caffeine and iv) outside the first hydration shell of caffeine.

Boole's rule and also applying a Hanning window. The normalized COM velocity TCF of caffeine and the oxygen (which is very close to the COM of water) velocity TCF of water are presented, together with the associated normalized spectral densities $S_v^i(\omega)/S_v^i(0)$, in Fig. 7. From this figure it can be clearly seen that the velocity TCF of caffeine and water molecules are quite different, something which is reflected on the low frequency intermolecular vibrations which are associated to the peaks of the corresponding spectral densities. The normalized spectral density corresponding to the COM of caffeine exhibits a peak located at 24 cm^{-1}, which corresponds to intermolecular vibrations due to cage effects [54]. In the case of water, this peak is shifted to 50 cm^{-1} which is an indication of the faster intermolecular vibrations in the case of water. In the literature, this peak around 50 cm^{-1} in the case of pure liquid water is attributed to underlying mechanisms arising from hydrogen bridge bonds and cage effects [55–59]. Moreover, as it is well known in liquid water [45], a shoulder around 204 cm^{-1} is observed. Previous experimental studies [60] have suggested that the intermolecular vibrations in this range of wavenumbers can be attributed to hindered translations of water molecules within a local tetrahedral HB network.

The effect of the HB interactions between water and caffeine on the translational dynamics of water molecules have also been studied. To do so, the normalized oxygen velocity TCF and corresponding normalized spectral densities of water molecules which at t = 0 are i) hydrogen-bonded with O1 of caffeine, ii) hydrogen-bonded with O2 of caffeine, iii) hydrogen-bonded with N4 of caffeine and iv) outside the first hydration shell of caffeine, were calculated and are depicted in Fig. 8. From these figures it can be seen that due to the interaction of water with caffeine, the translational dynamics of water molecules become more hindered. More specifically, the negative local minimum around t = 0.08 ps observed in the velocity TCF exhibits more negative values when water molecules are initially hydrogen-bonded with caffeine in comparison with those which a t = 0 are outside the first hydration shell of caffeine. This is a clear indication of the more hindered translations of water molecules which are hydrogen bonded to caffeine. The formation of hydrogen bonds between water and caffeine is also very clearly reflected on the normalized spectral densities, which in the case of water molecules hydrogen bonded with caffeine exhibit a peak located around 175 cm^{-1}. These peaks are also significantly more pronounced when water forms hydrogen bonds with O1, O2, which as shown previously exhibit much longer lifetimes. In the case of weaker hydrogen bonds (such as the H_w … N4 ones) the calculated spectral density exhibits a low-intensity peak, which is also red-shifted to 149 cm^{-1}. On the other hand, these peaks are absent in the case of water molecules which are t = 0 are outside the first hydration shell. This is a clear indication that these intermolecular vibrations are associated to the HB interactions of water with caffeine.

The non-normalized COM velocity TCF can be also used to estimate the self-diffusion coefficient of caffeine and water, using the well-known Green-Kubo relation:

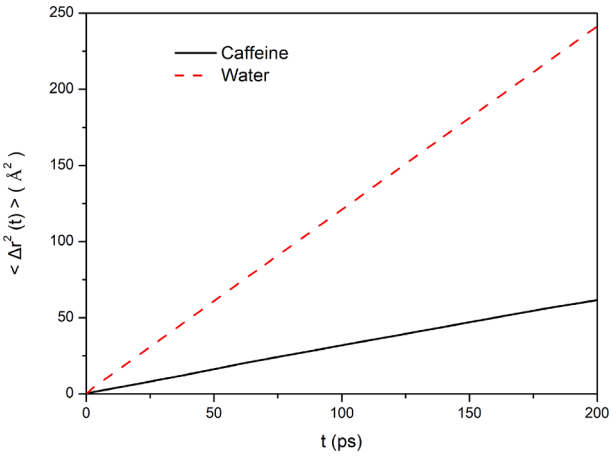

Fig. 9. Calculated COM mean square displacements for caffeine and water molecules.

$$D_i = \frac{1}{3}\cdot\int_0^{\infty}\left\langle \vec{v}_i(0)\cdot\vec{v}_i(t)\right\rangle\cdot dt \tag{8}$$

Alternatively, the self-diffusion coefficient of caffeine and water can be calculated using the calculated molecular mean-square displacements (MSD) and the well-known Einstein relation:

$$D_i = \frac{1}{6}\lim_{t\to\infty}\frac{1}{t}\left\langle|\overrightarrow{\Delta r_i}(t)|^2\right\rangle = \frac{1}{6}\lim_{t\to\infty}\frac{1}{t}\left\langle|\vec{r_i}(0)-\vec{r_i}(t)|^2\right\rangle \tag{9}$$

The calculated MSD for caffeine and water molecules are presented in Fig. 9. The calculated values of the self-diffusion of caffeine and water using the Green-Kubo formalism were $D_{Caffeine} = 0.50\cdot10^{-9}m^2/s$ and $D_{Water} = 2.25\cdot10^{-9}m^2/s$. When using the Einstein relation, the corresponding calculated values were $D_{Caffeine} = 0.51\cdot10^{-9}m^2/s$ and $D_{Water} = 2.0\cdot10^{-9}m^2/s$. The experimentally reported values for the self-diffusion of caffeine diluted in water and pure liquid water are $D_{Caffeine} = 0.62\cdot10^{-9}m^2/s$ [61] and $D_{Water} = 2.299\cdot10^{-9}m^2/s$ [62,63], signifying that the employed potential models in our simulation predict the self-diffusion of caffeine and water with good accuracy.

3.4. Quantum chemical calculations

The geometry of the hydrated caffeine molecule was initially optimized using DFT calculations with the B3LYP and M06-2X functionals and the 6-31G(d,p) and Def2TZVP basis sets, including the water solvent implicitly as a dielectric continuum. The predicted geometry was almost the same in all cases, as expected. Subsequently, in order to include the solvent explicitly, the first hydration shell of the caffeine molecule, containing caffeine and 56 water molecules, was energetically optimized using the DFT and at ONIOM multi-scale methodologies. The geometrically optimized caffeine molecule and the water molecules in the first hydration shell of caffeine are depicted in Fig. 10 and some of the most representative features of the intra- and inter-molecular geometrical characteristics of caffeine and its HB dimers with the surrounding water molecules are presented in Table 2. The ONIOM(DFT:PM6) methodologies predict the formation of three hydrogen bonds per caffeine molecule, similarly to the MD simulations. Due to the formation of these hydrogen bonds, the C = O bonds in the quantum chemical calculations are slightly elongated up to 0.03 Å. The predicted hydrogen bond lengths also range from 1.82 Å to 1.97 Å (Table 2). In general, we may say that the general geometrical characteristics of the first hydration shell of caffeine are very similar, independently if they have been predicted in the framework of the MD simulations or with the ONIOM methodology. Note also that the results obtained when using the M06-2X functional are in better agreement with the ones predicted by the MD simulations.

The interaction energy of the caffeine molecule with its first hydration sphere is calculated at the geometry obtained via the MD simulations and at the ONIOM(DFT:PM6) methodology. For the calculation of the interaction energy the whole hydration shell of caffeine, i.e., caffeine and the 56 water molecules, was taken into account in the calculations,

Table 2
C = O bond distances in Å, intermolecular distances between the hydrogen atom of water molecules and O_1, O_2 and N_4 atoms of caffeine in Å.

	Method [a]	C = O_1	C = O_2	H_w... O_1	H_w... O_2	H_w... N_4
Caffeine	B3LYP/1	1.228	1.232			
	B3LYP/2	1.224	1.227			
	M06-2X/1	1.222	1.224			
	M06-2X/2	1.219	1.220			
Caffeine in W [b]		1.213	1.215	1.644	1.745	1.930
Caffeine@W_{56} [c]	B3LYP/1	1.243	1.242	1.958	1.840	2.212
	B3LYP/2	1.243	1.233	1.902	1.859	1.978
	M06-2X/1	1.248	1.229	1.823	1.874	1.978
	M06-2X/2	1.238	1.223	1.892	1.815	1.968

[a] 1:6-31G(d,p); 2:Def2TZVP.
[b] Structure obtained from the MD simulations in this study.
[c] Structure obtained from the ONIOM calculations.

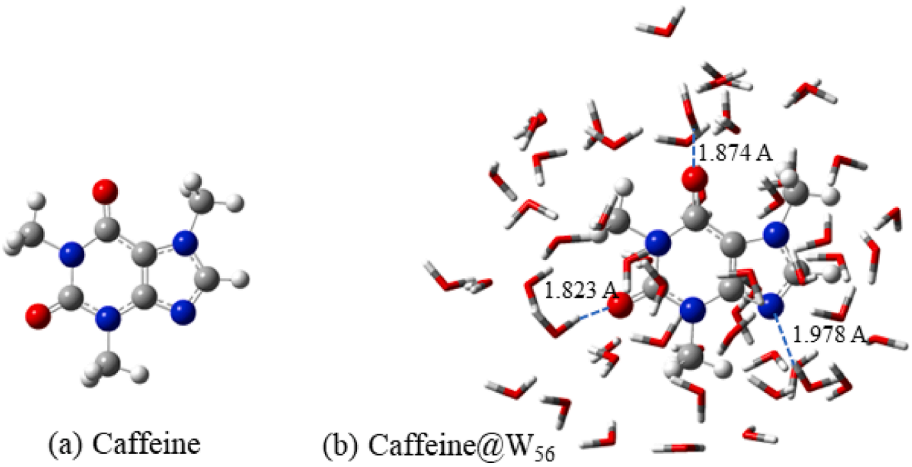

Fig. 10. Minimum energy calculated structures at M06-2X/6-31G(d,p) of Caffeine and of caffeine in the first hydration shell containing 56 water molecules.

Table 3
Interaction energies in kcal/mol of caffeine with its 1st hydration sphere of 56 water molecules with (ΔE) and without BSSE (ΔE_u) corrections and the deformation energy of caffeine (Def) in kcal/mol at B3LYP/6-31G(d,p) and B3LYP/Def2TZVP.

Basis Set	ΔE_u	ΔE	Def	ΔE_u	ΔE	Def
ONIOM geometry				*MD geometry*		
6-31G(d,p)	−54.7	−18.0	9.4	−46.4	−20.4	8.3
Def2TZVP	−21.3	−14.3	10.3	−21.7	−16.8	9.2

which were performed at the DFT(B3LYP and M06-2X) level of theory and using two basis sets, (6-31G(d,p) and Def2TZVP). The interaction energy has been corrected with respect to the basis set superposition error (BSSE) [64,65] which results from the fact that the basis set is not infinite. The small 6-31G(d,p) basis set has a large BSSE. However, both basis sets predict similar interaction BSSE corrected energies, as it can be seen in Table 3. We conclude that the interaction energy is −14.3 kcal/mol. The calculated deformation energy of the caffeine due to the interaction of the water molecules, i.e., the energy demands for the geometry changes due to interaction of the water molecules with the caffeine molecule, is 10.3 kcal/mol, as depicted in Table 3.

Generally, in quantum calculations, the solvent is included implicitly for reason of simplicity. However, it has been shown that the explicit inclusion of the solvent molecules may affect significantly both absorption and emission spectra depending on the solute and on the interaction of solute with the solvent [66,67]. Thus, in the present study the effect of the explicit inclusion of the 1st solvation spere on the caffeine absorption and emission spectra is examined. The absorption spectrum of caffeine including the solvent explicitly, implicitly, and both explicitly and implicitly (as described in section 2) using different methodologies is depicted in Fig. 11. The first solvation sphere of 56 water molecules has been included via DFT methodology and via the multi-scale ONIOM methodology. The λ_{max}, energy differences (ΔE), and oscillator strength (f-values), of the main absorption peaks of Caffeine and of the Caffeine@W56 are given in Table 4.

All methodologies predict the same general shape of the absorption spectra, as it can be seen in Fig. 11. It is found that the B3LYP functional predicts the main peak at about 266 nm, in excellent agreement with the experimental values of 272.9 and 273.0 nm for low concentration aqueous solutions of caffeine [9,68], i.e., the B3LYP peak is only 7 nm blue shifted when compared to the experimental values. On the contrary, the M06-2X functional predicts a larger shift of this peak, i.e., the M06-2X peak is about 30 nm blue shifted when compared to the experimental value.

The 1st main peak corresponds to a HOMO → LUMO (H → L) excitation, depicted in Fig. 12. It is interesting that a small part of electron density is localized around the water molecules which exhibit strong van der Waals interactions with caffeine, as depicted in the HOMO orbitals. Furthermore, it is found that all approaches, i.e., explicit, implicit, and both explicit and implicit inclusion of water solvent, predict almost the same λ_{max} and f-oscillator strength values. The B3LYP λ_{max} ranges from 259 nm to 266 nm depending on the approach of the inclusion of the water solvent, as shown in Table 4. Moreover, it should be noted that the 6-31G(d,p) and Def2TZVP basis sets predict the same data for the main peak. Finally, the calculated absorption spectrum, predicts other two major peaks at about 210 nm and 190 nm (see Table 4), in excellent

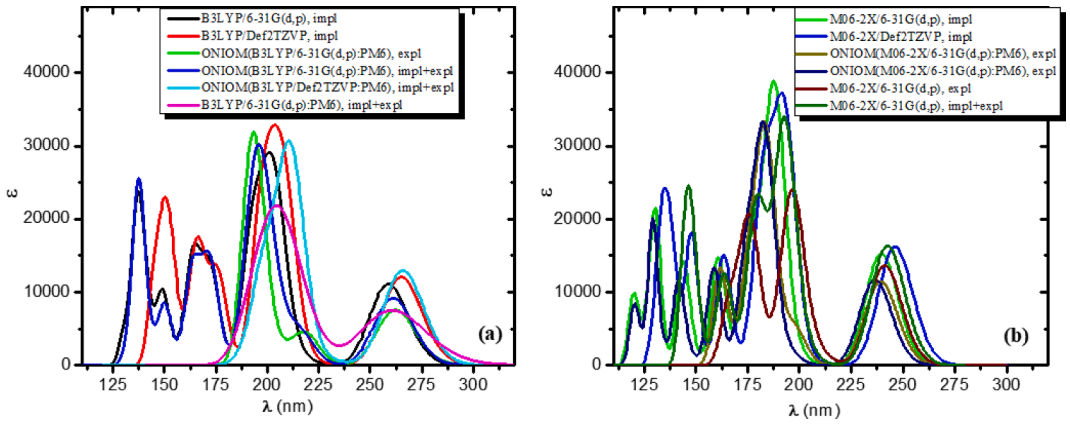

Fig. 11. Absorption spectra of caffeine in water, using different approaches for the inclusion of the water solvent.

Table 4
Absorption main peaks, λ (nm), energy differences, ΔE (eV), and f-values of the caffeine and of the Caffeine@W_{56} at different levels of theory.

Methodology	Solvent	Geom	λ_{max} [a]	ΔE	f	λ_{max} [b]	ΔE	f	λ_{max} [c]	ΔE	f
Caffeine											
B3LYP/6-31G(d,p)	Impl	opt	258.7	4.793	0.164	203.4	6.096	0.349	192.3	6.449	0.225
B3LYP/Def2TZVP	Impl	opt	265.0	4.679	0.179	207.8	5.967	0.367	197.5	6.278	0.259
M06-2X/6-31G(d,p)	Impl	opt	239.6	5.174	0.226	188.2	6.587	0.530	160.8	7.111	0.214
M06-2X/Def2TZVP	Impl	opt	246.2	5.036	0.241	193.1	6.421	0.480	183.8	6.745	0.295
Caffeine@W_{56}											
ONIOM(B3LYP/6-31G(d,p):PM6	expl	opt	262.2	4.783	0.112				192.2	6.452	0.332
ONIOM(B3LYP/6-31G(d,p):PM6	impl + expl	opt	260.9	4.752	0.136	197.6	6.276	0.288	171.2	7.242	0.128
ONIOM(B3LYP/Def2TZVP:PM6)	impl + expl	MD	265.9	4.443	0.192	212.1	5.846	0.362			
ONIOM(M06-2X/6-31G(d,p):PM6	expl	opt	240.2	5.162	0.173	183.3	6.764	0.348	175.2	7.075	0.185
ONIOM(M06-2X/6-31G(d,p):PM6	impl + expl	opt	239.6	5.174	0.200	185.9	6.669	0.498	174.5	7.105	0.176
ONIOM(M06-2X/6-31G(d,p):PM6	expl	MD	236.6	5.239	0.175	183.7	6.749	0.369	174.3	7.115	0.213
B3LYP/6-31G(d,p)	impl + expl	opt	260.5	4.759	0.185	208.3	5.951	0.243			
M06-2X/6-31G(d,p)	expl	MD	241.3	5.139	0.203	197.0	6.295	0.330	176.4	7.027	0.152
M06-2X/6-31G(d,p)	impl + expl	MD	242.6	5.111	0.243	192.9	6.427	0.490	180.7	6.862	0.255
Expt [d]			272.90								

[a] $S_0 \rightarrow S_1$, 0.97|H → L >. [b] |H → L + 1 >. [c] |H → L + 2 >. [d] Ref.[9].

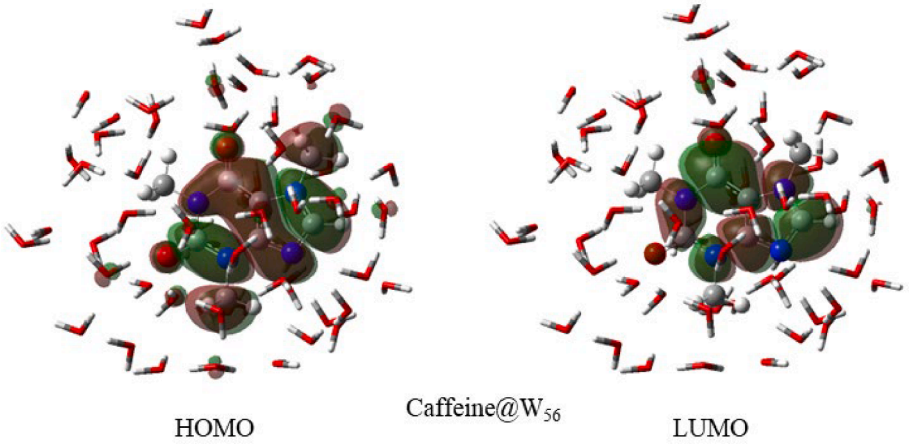

Fig. 12. The HOMO(H) and LUMO(L) orbitals of the Caffeine@W_{56} cluster.

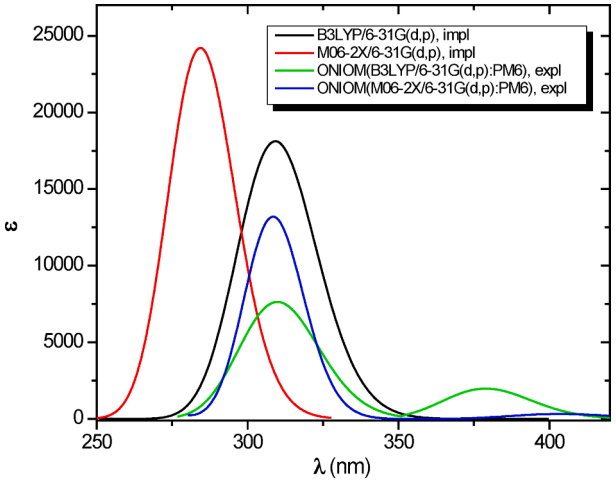

Fig. 13. Emission spectra of caffeine in water, using different methodologies and approaches for the inclusion of the water solvent.

Table 5
Emission peaks of the $S_x \rightarrow S_0$ de-excitation, λ (nm), energy differences, ΔE (eV), and f-values of the caffeine and of the Caffeine@W_{56} at different levels of theory.

Methodology	Solvent	λ_{max}	ΔE	f
Caffeine				
B3LYP/6-31G(d,p)	impl	309.2 [a]	4.010	0.269
M06-2X/6-31G(d,p)	impl	284.4 [a]	4.360	0.359
Caffeine@W_{56}				
ONIOM(B3LYP/6-31G(d,p):PM6	expl	386.5 [a]	3.208	0.022
ONIOM(B3LYP/6-31G(d,p):PM6	expl	309.9[b]	4.000	0.113
ONIOM(M06-2X/6-31G(d,p):PM6	expl	390.8 [a]	3.173	0.004
ONIOM(M06-2X/6-31G(d,p):PM6	expl	308.5[b]	4.019	0.145
Expt [c]		386.0		

[a] $S_1 \rightarrow S_0$. [b] $S_2 \rightarrow S_0$. [c] Ref. [9].

agreement with the previous DFT calculated absorption spectra of Gómez et al and the available experimental value of 205 nm [19,68].

The emission spectrum of caffeine is plotted in Fig. 13 and the λ values, energy differences, ΔE (eV), and f-values are given in Table 5. While for the calculation of the absorption spectrum the inclusion of the solvent both explicitly and implicitly results in the same spectra, for the correct calculation of the emission spectra the explicit inclusion of the solvent is necessary. Both B3LYP and M06-2X functionals predict a peak at 387 and 391 nm in excellent agreement with the experimental value of 386.0 nm [9]. On the contrary, when the solvent is included implicitly only, the fluorescence peak is at 309 nm (B3LYP) and 284 nm (M06-2X).

It should be noted that the first emitting peak at 387 nm corresponds to the $S_1 \rightarrow S_0$ de-excitation and has a small oscillator strength. The geometry optimization of the 1st excited state results to an elongation of the C = O bond and in a shorter HOH…O = C intermolecular distance, see Fig. 14a. On the contrary, the second emission peak that is at 310 nm is more intense than the 1st peak, corresponds to the $S_2 \rightarrow S_0$ de-excitation and the optimized geometry of the second excited state is similar to the ground state of the caffeine molecule. The two peaks correspond to a H → L and H-1 → L, see Fig. 14b. Both H-1 and H orbitals have electron density on the water molecules that interact with the caffeine. The water HB network inside the first hydration shell of caffeine is also depicted.

4. Conclusions

In the framework of the present study, a multi-scale approach involving classical MD simulations and quantum chemical calculations has been employed in order to study the hydration structure and related dynamics of caffeine diluted in liquid water, as well as to calculate the UV–Vis and fluorescence emission spectra of hydrated caffeine.

The results obtained have revealed that the first hydration shell of caffeine, which has a radius of 7.68 Å, consists on average of 56 water molecules. Moreover, in the predominant local hydration structures of caffeine, caffeine forms three hydrogen bonds with its neighbour water molecules, acting as a hydrogen bond acceptor. Among these hydrogen bonds, the O1 … H_W and O2 … H_W ones persist for a longer time-scale, as reflected on the decay and the corresponding lifetimes of the calculated continuous and intermittent HB TCF.

The reorientation of hydrated caffeine is also much slower in comparison with water, leading to an order of magnitude difference in the calculated reorientational correlation times of caffeine and water. Additionally, the HB interactions of water molecules with caffeine promote more abrupt changes in the short-time reorientational dynamics of water, causing a more hindered rotation of water molecules which interact with caffeine.

The existence of HB interactions between water and caffeine also affects their translational dynamics, as reflected on the shape of the calculated velocity TCF and the low-frequency peaks of the corresponding spectral densities, revealing more hindered translations of water molecules when they are hydrogen bonded to caffeine. The calculated self-diffusion coefficients also reveal a much slower diffusivity of caffeine in comparison with water, a result in agreement with available experimental data.

Both the classical MD and DFT methodologies predict that caffeine forms three hydrogen bonds with its closest water neighbour molecules. The DFT calculations have predicted that the formation of these

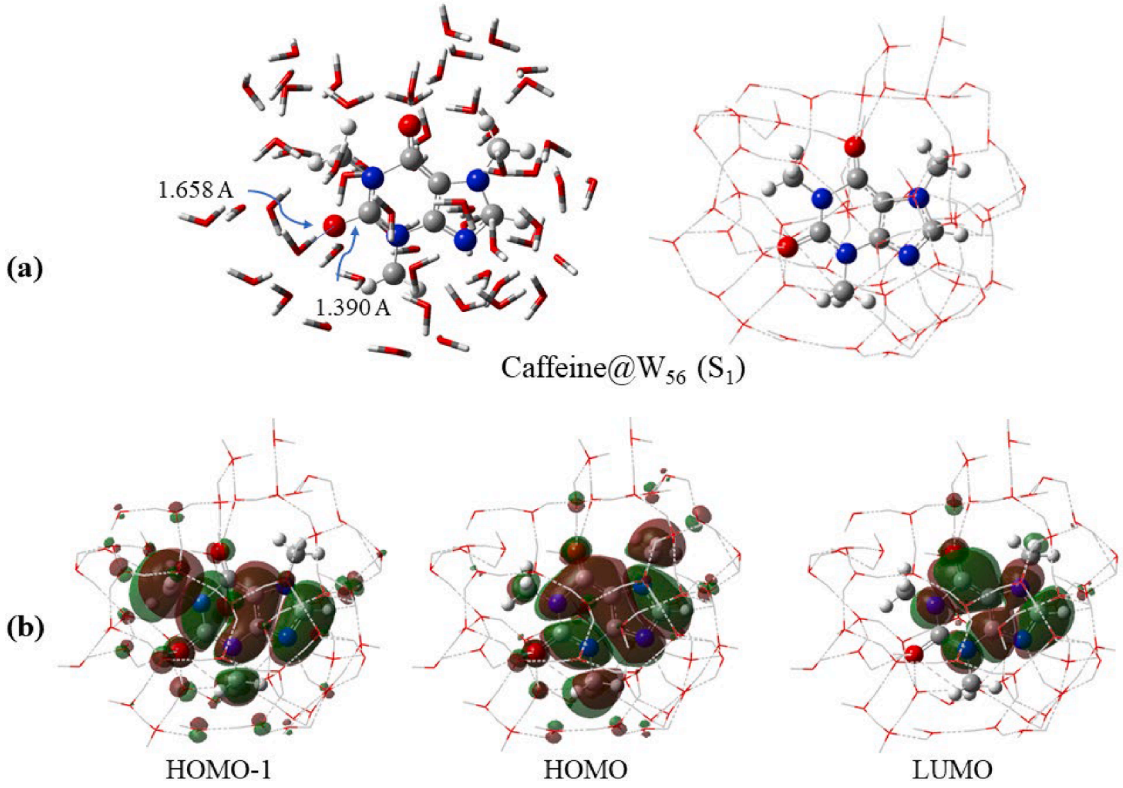

Fig. 14. **(a)** S_1 minimum energy structure of caffeine in water. The water HB network inside the first hydration shell is also depicted. **(b)** The H-1, H and L orbitals of the Caffeune@W_{56} cluster at the S_1 optimized geometry.

hydrogen bonds slightly elongates the C = O bonds of caffeine. They also have predicted that the interaction energy of caffeine with the water molecules is −14.3 kcal/mol. Interestingly, according to the DFT calculations, a small part of electron density is localized around the water molecules which exhibit strong van der Waals interactions with caffeine, as depicted in the calculated HOMO orbitals.

All approaches in the TD-DFT calculations for the inclusion of the water solvent, i.e., explicit, implicit, and both explicit and implicit, predict almost the same λ_{max} and f-oscillator strength values. The B3LYP functional predicts the main peak at about 266 nm, in excellent agreement with the experimental value of 272.9 nm. While for the calculation of the absorption spectrum, the inclusion of the solvent both explicitly and implicitly results in the same spectra, for the correct calculation of the emission spectra the explicit inclusion of the solvent is necessary. Both B3LYP and M06-2X functionals predict a peak at 387 and 391 nm in excellent agreement with the experimental value of 386.0 nm.

The results obtained in the framework of the present study might considered as a springboard and a first approach towards a further development of multi-scale computational protocols in order to determine hydration structure and dynamics and their interrelation with electronic spectra of alkaloids in water, aiming to provide in the near future a link between theoretical physical chemistry and analytical chemistry applications. Further work on this topic is in progress.

Declaration of Competing Interest

The authors declare that they have no known competing financial interests or personal relationships that could have appeared to influence the work reported in this paper.

Data availability

Data will be made available on request.

References

[1] N.P. Rodrigues, N. Bragagnolo, Identification and quantification of bioactive compounds in coffee brews by HPLC–DAD–MS, J. Food Compos. Anal. 32 (2013) (2013) 105–115.
[2] A. Nehlig, J.L. Daval, G. Debry, Caffeine and the central nervous system: mechanisms of action, biochemical, metabolic and psychostimulant effects, Brain Res. Rev. 17 (1992) 139–170.
[3] M.M. Karim, C.W. Jeon, H.S. Lee, S.M. Alam, S.H. Lee, J.H. Choi, S.O. Jin, A.K. Das, Simultaneous Determination of Acetylsalicylic Acid and Caffeine in Pharmaceutical Formulation by First Derivative Synchronous Fluorimetric Method, J. Fluoresc. 16 (2006) 713–721.
[4] T.M. McLellan, J.A. Caldwell, H.R. Lieberman, A review of caffeine's effects on cognitive, physical and occupational performance, Neurosci. Biobehav. Rev. 71 (2016) 294–312.
[5] A. Baratloo, A. Rouhipour, M.M. Forouzanfar, S. Safari, M. Amiri, A. Negida, The role of caffeine in pain management: A brief literature review, Anesth. Pain Med. 6 (2016) e33193.
[6] F. Fritz, R. Preissner, P. Banerjee, VirtualTaste: A web server for the prediction of organoleptic properties of chemical compounds, Nucleic Acids Res. 49 (2021) W679–W684.
[7] A. Herman, A.P. Herman, Caffeine's mechanisms of action and its cosmetic use, Skin Pharmacol. Physiol. 26 (2013) 8–14.
[8] M.B. Pimparade, J.T. Morott, J.-B. Park, V.I. Kulkarni, S. Majumdar, S.N. Murthy, Z. Lian, E. Pinto, V. Bi, T. Durig, R. Murthy, H.N. Shivakumar, K. Vanaja, P. C. Kumar, M.A. Repka, Development of taste masked caffeine citrate formulations utilizing hot melt extrusion technology and in vitro-in vivo evaluations, Int. J. Pharm. 487 (2015) 167–176.
[9] H. Yisak, M. Redi-Abshiro, B.S. Chandravanshi, New fluorescence spectroscopic method for the simultaneous determination of alkaloids in aqueous extract of green coffee beans, Chem. Cent. J. 12 (2018) 59.
[10] S.E. Sheppard, The effects of environment and aggregation on the absorption spectra of dyes, Rev. Mod. Phys. 14 (1942) 303–340.
[11] M. Noboru, K. Yozo, K. Masao, The solvent effect on fluorescence spectrum, change of solute-solvent interaction during the lifetime of excited solute molecule, Bull. Chem. Soc. Jpn 28 (1955) 690–691.
[12] S. Abou-Hatab, V. Carnevale, S. Matsika, Modeling solvation effects on absorption and fluorescence spectra of indole in aqueous solution, J. Chem. Phys. 154 (2021) 064104.
[13] I. Skarmoutsos, G. Maurin, E. Guardia, J. Samios, Hydration structure and dynamics of the favipiravir antiviral drug: A molecular modelling approach, Bull. Chem. Soc. Jpn 93 (2020) 1378–1385.
[14] M.P. Allen, D.J. Tildesley, Computer simulations of liquids, Oxford University Press, Oxford, 1987.

[15] D.R. Salahub, Multiscale molecular modelling: From electronic structure to dynamics of nanosystems and beyond, PCCP 24 (2022) 9051–9081.
[16] I. Skarmoutsos, I.D. Petsalakis, J. Samios, The polar cosolvent effect on caffeine solvation in supercritical CO_2-ethanol mixtures: A molecular modeling approach, Ind. Eng. Chem. Res. 60 (2021) 11834–11847.
[17] J.L.F. Abascal, C. Vega, A general purpose model for the condensed phases of water: TIP4P/2005, J. Chem. Phys. 123 (2005) 234505.
[18] C.D. Zeinalipour-Yazdi, A DFT study of the interaction of aspirin, paracetamol and caffeine with one water molecule, J. Mol. Model. 28 (2022) 285.
[19] S. Gómez, T. Giovannini, C. Cappelli, Absorption Spectra of Xanthines in Aqueous Solution: A Computational Study, PCCP 22 (2020) 5929–5941.
[20] V.B. Singh, Spectroscopic signatures and structural motifs in isolated and hydrated caffeine: A computational study, RSC Adv. 4 (2014) 58116–58126.
[21] R. Sanjeewa, S. Weerasinghe, Development of a molecular mechanics force field for caffeine to investigate the interactions of caffeine in different solvent media, J. Mol. Struc.-THEOCHEM 944 (2010) 116–123.
[22] L. Bondesson, K.V. Mikkelsen, Y. Luo, P. Garberg, H. Ågren, Hydrogen bonding effects on infrared and Raman spectra of drug molecules, Spectrochim. Acta A Mol. Biomol. Spectrosc. 66 (2007) 213–224.
[23] L. Tavagnacco, U. Schnupf, P.E. Mason, M.-L. Saboungi, A. Cesàro, J.W. Brady, Molecular dynamics simulation studies of caffeine aggregation in aqueous solution, J. Phys. Chem. B 115 (2011) 10957–10966.
[24] R. Sanjeewa, S. Weerasinghe, Study of aggregate formation of caffeine in water by molecular dynamics simulation, Comput Theor. Chem. 966 (2011) 140–148.
[25] L. Tavagnacco, Y. Gerelli, A. Cesàro, J.W. Brady, Stacking and branching in self-aggregation of caffeine in aqueous solution: From the supramolecular to atomic scale clustering, J. Phys. Chem. B 120 (2016) 9987–9996.
[26] L. Tavagnacco, J.W. Brady, F. Bruni, S. Callear, M.A. Ricci, M.-L. Saboungi, A. Cesàro, Hydration of caffeine at high temperature by neutron scattering and simulation studies, J. Phys. Chem. B 119 (2015) 13294–13301.
[27] W. Smith, T.R. Forester, DL_POLY_2.0: A general-purpose parallel molecular dynamics simulation package, J. Mol. Graph. 14 (1996) 136–141.
[28] L. Martínez, R. Andrade, E.G. Birgin, J.M. Martínez, PACKMOL: A package for building initial configurations for molecular dynamics simulations, J. Comput. Chem. 30 (2009) 2157–2164.
[29] W.G. Hoover, Canonical dynamics: Equilibrium phase-space distributions, Phys. Rev. A 31 (1985) 1695–1697.
[30] W.G. Hoover, Constant-pressure equations of motion, Phys. Rev. A 34 (1986) 2499–2500.
[31] C.T. Lee, W.T. Yang, R.G. Parr, Development of the Colle-Salvetti correlation-energy formula into a functional of the electron density, Phys. Rev. B: Condens. Matter Mater. Phys. 37 (1988) 785–789.
[32] A.D. Becke, A new mixing of hartree-fock and local density-functional theories, J. Chem. Phys. 38 (1993) 1372–1377.
[33] Y. Zhao, D.G. Truhlar, The M06 suite of density functionals for main group thermochemistry, thermochemical kinetics, noncovalent interactions, excited states, and transition elements: Two new functionals and systematic testing of four M06-class functionals and 12 other functionals, Theor. Chem. Acc. 120 (2008) 215–241.
[34] L.A. Curtiss, M.P. McGrath, J.P. Blaudeau, N.E. Davis, R.C. Binning, L. Radom, Extension of gaussian-2 theory to molecules containing third-row atoms Ga-Kr, J. Chem. Phys. 103 (1995) 6104–6113.
[35] F. Weigend, R. Ahlrichs, Balanced basis sets of split valence, triple zeta valence and quadruple zeta valence quality for H to Rn: Design and assessment of accuracy, PCCP 7 (2005) 3297–3305.
[36] S. Miertuš, E. Scrocco, J. Tomasi, Electrostatic interaction of a solute with a continuum. A direct utilization of AB initio molecular potentials for the prevision of solvent effects, Chem. Phys. 55 (1981) 117–129.
[37] J. Tomasi, B. Mennucci, R. Cammi, Quantum mechanical continuum solvation models, Chem. Rev. 105 (2005) 2999–3094.
[38] S. Dapprich, I. Komáromi, K.S. Byun, K. Morokuma, M.J. Frisch, A new ONIOM implementation in gaussian 98. 1. The calculation of energies, gradients and vibrational frequencies and electric field derivatives, J. Mol. Struct. (THEOCHEM) 462 (1999) 1–21.
[39] M.J. Frisch G.W. Trucks H.B. Schlegel G.E. Scuseria M.A. Robb J. R. Cheeseman G. Scalmani V. Barone B. Mennucci G. A. Petersson et al. Gaussian 16, Revision C.01; Gaussian, Inc.: Wallingford, CT, USA, 2016.
[40] J. Martí, J.A. Padro, E. Guàrdia, Molecular dynamics simulation of liquid water along the coexistence curve: Hydrogen bonds and vibrational spectra, J. Chem. Phys. 105 (1996) 639–649.
[41] A. Luzar, D. Chandler, Structure and hydrogen bond dynamics of water–dimethyl sulfoxide mixtures by computer simulations, J. Chem. Phys. 98 (1993) 8160–8173.
[42] P. Jedlovszky, I. Bakó, G. Pálinkás, T. Radnai, A.K. Soper, Investigation of the uniqueness of the reverse monte carlo method: Studies on liquid water, J. Chem. Phys. 105 (1996) 245–254.
[43] M. Canales, E. Guàrdia, Computer simulation study of ion-water and water-water hydrogen bonds in sulfuric acid solutions at low temperatures, J. Mol. Liq. 347 (2022) 118351.
[44] O. Gereben, L. Pusztai, Hydrogen bond connectivities in water–ethanol mixtures: On the influence of the H-bond definition, J. Mol. Liq. 220 (2016) 836–841.
[45] I. Skarmoutsos, G. Franzese, E. Guàrdia, Using Car-Parrinello simulations and microscopic order descriptors to reveal two locally favored structures with distinct molecular dipole moments and dynamics in ambient liquid water, J. Mol. Liq. 364 (2022) 119936.
[46] J. Russo, H. Tanaka, Understanding water's anomalies with locally favoured structures, Nat. Commun. 5 (2014) 3556.
[47] I. Skarmoutsos, E. Guardia, J. Samios, Hydrogen bond, electron donor-acceptor dimer, and residence dynamics in supercritical CO_2-ethanol mixtures and the effect of hydrogen bonding on single reorientational and translational dynamics: A molecular dynamics simulation study, J. Chem. Phys. 133 (2010) 014504.
[48] J.A. Padro, L. Saiz, E. Guàrdia, Hydrogen bonding in liquid alcohols: A computer simulation study, J. Mol. Struct. 416 (1997) 243–248.
[49] I. Skarmoutsos, E. Guardia, Local structural effects and related dynamics in supercritical ethanol. 2. Hydrogen-bonding network and its effect on single reorientational dynamics, J. Phys. Chem. B 113 (2009) 8898–8910.
[50] F.W. Starr, J.K. Nielsen, H.E. Stanley, Hydrogen-bond dynamics for the extended simple point-charge model of water, Phys. Rev. E 62 (2000) 579–587.
[51] D. Laage, J.T. Hynes, A molecular jump mechanism of water reorientation, Science 311 (2006) 832–835.
[52] R. Ludwig, The mechanism of the molecular reorientation in water, ChemPhysChem 8 (2007) 44–46.
[53] D. Laage, J.T. Hynes, On the molecular mechanism of water reorientation, J. Phys. Chem. B 112 (2008) 14230–14242.
[54] E. Guardia, I. Skarmoutsos, M. Masia, Hydrogen bonding and related properties in liquid water: A car-parrinello molecular dynamics simulation study, J. Phys. Chem. B 119 (2015) 8926–8938.
[55] M. Galvin, D. Zerulla, The extreme low-frequency raman spectrum of liquid water, ChemPhysChem 12 (2011) 913–914.
[56] K.H. Tsai, W. Ten-Ming, Local structural effects on low-frequency vibrational spectrum of liquid water: The instantaneous-normal-mode analysis, Chem. Phys. Lett. 417 (2006) 389–394.
[57] J.A. Padro, J. Marti, An interpretation of the low-frequency spectrum of liquid water, J. Chem. Phys. 118 (2003) 452–453.
[58] A. De Santis, A. Ercoli, D. Rocca, Comment on "An Interpretation of the Low-Frequency Spectrum of Liquid Water", J. Chem. Phys. 120 (2004) 1657–1658.
[59] J.A. Padro, J. Marti, Response to comment on "An Interpretation of the Low-Frequency Spectrum of Liquid Water", J. Chem. Phys. 120 (2004) 1659–1660.
[60] R. Schwan, C. Qu, D. Mani, N. Pal, G. Schwaab, J.M. Bowman, G.S. Tschumper, M. Havenith, Observation of the low-frequency spectrum of the water trimer as a sensitive test of the water-trimer potential and the dipole-moment surface, Angew. Chem. Int. Ed. 59 (2020) 11399–11407.
[61] S.V. Blokhina, T.V. Volkova, V.A. Golubev, G.L. Perlovich, Understanding of relationship between phospholipid membrane permeability and self-diffusion coefficients of some drugs and biologically active compounds in model solvents, Mol. Pharm. 14 (2017) 3381–3390.
[62] M. Holz, S.R. Heil, A. Sacco, Temperature-dependent self-diffusion coefficients of water and six selected molecular liquids for calibration in accurate ^{1}H NMR PFG measurements, PCCP 2 (2000) 4740–4742.
[63] R. Mills, Self-diffusion in normal and heavy water in the range 1–45°, J. Phys. Chem. 77 (1973) 685–688.
[64] S.F. Boys, F. Bernardi, Calculation of small molecular interactions by differences of separate total energies - Some procedures with reduced errors, Mol. Phys. 19 (1970) 553–566.
[65] S. Simon, M. Duran, J.J. Dannenberg, How does basis set superposition error change the potential surfaces for hydrogen-bonded dimers? J. Chem. Phys. 105 (1996) 11024–11031.
[66] D. Tzeli, I.D. Petsalakis, G. Theodorakopoulos, The solvent effect on a styryl-bodipy derivative functioning as an AND molecular logic gate, Inter. J. Quantum Chem. 120 (2020) e26181.
[67] C.E. Tzeliou, D. Tzeli, 3-input AND molecular logic gate with enhanced fluorescence output: The key atom for the accurate prediction of the spectra, J. Chem. Inf. Model. 62 (2022) 6436–6448.
[68] J. Chen, B. Kohler, Ultrafast nonradiative decay by hypoxanthine and several methylxanthines in aqueous and acetonitrile solution, PCCP 14 (2012) 10677–10682.